Remote In-Building Motion Detection Using Single Frequency Technique

R. Bonjour*, S. Welschen* and P. Leuchtmann and J. Leuthold
ETH Zurich, Institute of Electromagnetic Fields
Gloriastrasse 35, CH-8092 Zurich
SWITZERLAND

romain.bonjour@ief.ee.ethz.ch

P. Wellig
armasuisse Science and Technology
Feuerwerkerstrasse 39, CH-3602 Thun
SWITZERLAND

A new method for simple and robust in-building motion detection is introduced. The proposed technique relies on a single frequency continuous wave (CW) signal and can therefore be integrated with inexpensive commercial off-the-shelf (COTS) components.

INTRODUCTION

Remote sensing of building interiors, or through-the-wall sensing (TTWS), is of great interest for security and rescue applications [1]-[10]. Indeed, many applications ranging from detection of illegal activities to localization of people in rescue situations leverage TTWS. Over the past few years, several products fulfilling these needs have entered the market. In parallel, multiple research groups are working on further improving the performance of those systems. The potential enhancements to TTWS systems relate to higher sensitivity, higher accuracy, multiple target detection, or achievable standoff distance from the wall. However, these improvements usually come at the price of higher complexity and thus larger and more expensive setups with less battery service life.

TTWS research prototypes can be categorized into active and passive systems. In active sensing, the systems generate their own source signal in a way similar to radar systems. In the less common case of passive sensing, the systems use pre-existing signal sources such as mobile communication or radio signals. Recent works reported on phased array based active systems offering very good performance [11] or passive signs of life detection using Wi-Fi signals and phase extraction [12]. Indoor sensing has also been demonstrated using Doppler radar techniques [13]. Yet, none of these approaches focuses on simpler concepts enabling remote motion detection.

In this work, we introduce and demonstrate a robust active TTWS technique for remote in-building motion detection that is compatible with commercial off-the-shelf (COTS) components. The technique, called single frequency sensing (SFS) and based on ideas found in [14],[15], has the main advantage of being highly sensitive to movement variations while using low complexity hardware. Moreover, SFS should be deployable at tens of meters from the building, depending on the radiated power and the choice of antennas. In SFS, two transmitters generate continuous wave (CW) signals at a given frequency. One of the transmitters is then tuned in phase and amplitude in order to create destructive interference at the receiver. This procedure is called calibration and reduces the required dynamic range of the movement detector. After the calibration, small movements in the room in the order of a fraction of the wavelength of the continuous

* Both authors contributed equally to this work.

wave signal will affect the multipath channel and the phase of direct reflections and therefore the received amplitude at the receiver antenna.

The implementation of the proposed system ultimately requires only a sinusoidal waveform generation and a low speed acquisition board. Thanks to the high sensitivity of the proposed solution, we were able, in both simulations and experiments, remotely to detect motion through a brick wall in a room without using high-power amplifiers. The transmitted power in the waveform generator was set to $-2\mathrm{dBm}$. These results show that the proposed single frequency technique allows motion detection with low complexity hardware.

PRINCIPLE OF SINGLE FREQUENCY SENSING

As depicted on Figure 1, SFS rely on two transmitters T_1 and T_2 and a receiver. One transmitter, e.g. T_1, always sends the same CW signal. The second transmitter, e.g. T_2, is tuned in amplitude, phase, and polarization in order to produce destructive interference on the receiver. This is the calibration phase. If an object moves in the room afterward, the received signal will quickly increase, i.e. the "null" from the calibration process will be lost.

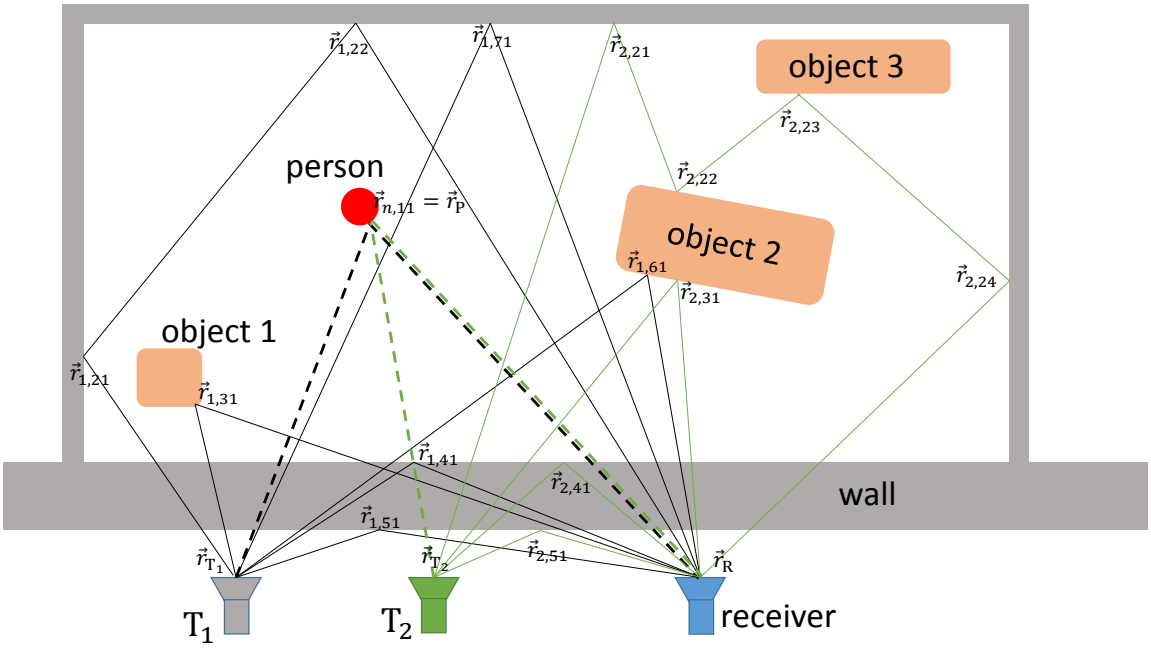

Figure 1: A subset of paths going out from the transmitters T_1 and T_2 make contributions to the receiver. Reflection points are marked with the position vectors $\vec{r}_{n,il}$. The paths that are due to reflections on the person are highlighted by the thick dashed lines. If the person is moving, mostly those fields that are reflected back from the person will change. Note that the true EM-waves fill the whole space while the path lines are merely part of the simplified model.

THEORY OF SINGLE FREQUENCY SENSING

In this section, the theory of SFS is explained in more detail in order to provide a fundamental understanding of the proposed concept. Two transmitters T_1 and T_2 (sending the complex signals x_1, x_2) and a receiver (receiving the complex signal y) are placed at some distance apart from each other on one side of a wall, see Figure 1. The receiver antenna is directed towards the wall. Ideally, it would be equally sensitive on the

full half sphere towards the wall in order to sense anything coming from beyond the wall. Further, to avoid interference from movements behind the system, the front-to-back ratio should be as high as possible.

Let $h_{1,2}$ be the transfer functions from the two transmitters to the receiver and let us assume that the transfer functions are of the same order of magnitude. In a stationary environment we have

$$y = h_1 x_1 + h_2 x_2 \tag{1}$$

with y being the complex received signal at the receiver and x_1 and x_2 the complex signal from transmitters T_1 and T_2, respectively.

Using a multipath formalism between the transmitters T_1, T_2 and the receiver (see Figure 1), we have

$$y = x_1 \sum_{i\text{th path}} h_{1i} + x_2 \sum_{j\text{th path}} h_{2j} = x_1 h_1 + x_2 h_2 \tag{2}$$

Let the number of paths from each of the transmitters be given by $P_n \geq 1$ ($n = 1,2$ refers to the transmitter) and let the ith path between the respective transmitter and receiver be composed of $L_{n,i}$ straight lines defined by the reflection points $\vec{r}_{n,il}$, $l = 0,1, \dots L_{n,i}$. Here, $\vec{r}_{n,i0} = \vec{r}_{T_n}$ is the location of the transmitter T_n and does not depend on the path number i while $\vec{r}_{n,iL_{n,i}} = \vec{r}_R$ is the location of the receiver which is the same for all paths. The length of the lth straight segment is given by $d_{n,il} = |\vec{r}_{n,il} - \vec{r}_{n,il-1}|, l = 1 \dots L_{n,i}$.

A typical partial transfer function h_{ni} might be (k is the wave number, which, for the sake of simplicity, is assumed constant for all segments)

$$\begin{aligned} h_{ni} &= \frac{e^{-jkd_{n,i1}}}{kd_{n,i1}} \prod_{l\text{th reflection}} c_{nil} \frac{e^{-jkd_{n,il+1}}}{kd_{n,il+1}} \\ &= e^{-jk\sum_{l=1}^{L_{n,i}} d_{n,il}} \prod_{l=1}^{L_{n,i}} \frac{c_{nil}}{kd_{n,il}}, \end{aligned} \tag{3}$$

where c_{nil} is the reflection coefficient at $\vec{r}_{n,il}$ and $c_{niL_{n,i}} = 1$ ($c_{niL_{n,i}}$ is the "reflection coefficient" of the last point along the path, i.e. the receiver). Note that from a physical point of view the given model includes some assumptions such as large distances (with respect to the wavelength) or small scattering objects. Otherwise the $1/kd$-behavior must be replaced. In fact, in a passive system each of the factors at the very right of the equation must be smaller than unity. Nevertheless, for our purposes, we can keep this model as given here.

In the following, we consider a scenario with a wall and some objects in the room behind it. The wall and the objects act as reflection points. In addition to this, there is a person to be detected in the room. This person acts as a yet unknown reflection point $\vec{r}_P$, which is part of exactly one single path from each transmitter. We choose the numbering such that this path is the first of all paths starting from a transmitter, i.e., $i, j = 1$ in the sum (2). Moreover, let the last segment of the path over $\vec{r}_P$ reach from the person to the receiver, i.e. $d_{n,1L_{n,1}} = |\vec{r}_R - \vec{r}_P|$. Suppose the person is located at the position $\vec{r}_P = \vec{r}_{P0}$. We keep the signal x_1 constant and tune x_2 such that $y = 0$. This tuning is possible without any knowledge of the structure of the transfer functions but merely by observing the received signal. In this state we have

$$x_2 = -\frac{h_1}{h_2} x_1. \tag{4}$$

Let us call this the calibration state of the system. As a result of the calibration process, the ratio

$$\frac{h_1(\vec{r}_{\mathrm{P}0})}{h_2(\vec{r}_{\mathrm{P}0})} = -\frac{x_2}{x_1} =: K_0 \tag{5}$$

is a known complex number. If the person moves, only the part h_{n1} of h_n will change. In the framework of (3) only a single reflection point is modified. In order to keep the formulae simple, we assume $L_{n,1} = 2$, i.e., the path over the person consists of only two segments. Then

$$\begin{aligned} h_{n1}(\vec{r}_{\mathrm{P}}) &= e^{-jk(|\vec{r}_{\mathrm{P}}-\vec{r}_{\mathrm{T}n}|+|\vec{r}_{\mathrm{R}}-\vec{r}_{\mathrm{P}}|)} \frac{c_n}{k^2|\vec{r}_{\mathrm{P}}-\vec{r}_{\mathrm{T}_n}||\vec{r}_{\mathrm{R}}-\vec{r}_{\mathrm{P}}|} \\ &= \frac{c_n e^{-jk|\vec{r}_{\mathrm{P}}-\vec{r}_{\mathrm{T}n}|}}{k|\vec{r}_{\mathrm{P}}-\vec{r}_{\mathrm{T}_n}|} \cdot \frac{e^{-jk|\vec{r}_{\mathrm{R}}-\vec{r}_{\mathrm{P}}|}}{k|\vec{r}_{\mathrm{R}}-\vec{r}_{\mathrm{P}}|}, \end{aligned} \tag{6}$$

where c_n is the reflection coefficient of the person for path n. The last form indicates that $h_{n1}(\vec{r}_{\mathrm{P}})$ can be seen as a signal coming from the person. The second factor contains no n.

The nth transfer function becomes

$$h_n(\vec{r}_{\mathrm{P}}) = h_{n1}(\vec{r}_{\mathrm{P}}) + \tilde{h}_n \tag{7}$$

where $\tilde{h}_n$ (the sum of all other paths) does not depend on the location of the person. For a large range of through-wall sensing applications we can assume that $h_{n1}(\vec{r}_{\mathrm{P}})$ (the direct reflection of the person which is highlighted in Figure 1) is small compared to $\tilde{h}_n$. This holds particularly due to the reflections from the wall.

Let $dh_n(\vec{r}_{\mathrm{P}})$ be the difference of the transfer functions when the person is located at an arbitrary point $\vec{r}_{\mathrm{P}}$ or at the calibration point $\vec{r}_{\mathrm{P}0}$ respectively:

$$dh_n(\vec{r}_{\mathrm{P}}) = h_n(\vec{r}_{\mathrm{P}}) - h_n(\vec{r}_{\mathrm{P}0}) = h_{n1}(\vec{r}_{\mathrm{P}}) - h_{n1}(\vec{r}_{\mathrm{P}0}) \tag{8}$$

It is important to note that this quantity includes only information about the direct path, which is highlighted in Figure 1. Assuming a known reflection coefficient c_n the complex value $dh_n(\vec{r}_{\mathrm{P}})$ varies with $\vec{r}_{\mathrm{P}}$ in a well-defined manner and can be formally evaluated using (6). Once the system is calibrated with the person at position $\vec{r}_{\mathrm{P}0}$, the person at position $\vec{r}_{\mathrm{P}} \neq \vec{r}_{\mathrm{P}0}$ generates the nonzero signal

$$\begin{aligned} y(\vec{r}_{\mathrm{P}}) &= \big(h_1(\vec{r}_{\mathrm{P}0}) + dh_1(\vec{r}_{\mathrm{P}})\big) \cdot x_1 + \big(h_2(\vec{r}_{\mathrm{P}0}) + dh_2(\vec{r}_{\mathrm{P}})\big) \cdot x_2 \\ &= \big(dh_1(\vec{r}_{\mathrm{P}}) - K_0 dh_2(\vec{r}_{\mathrm{P}})\big) \cdot x_1 =: dh(\vec{r}_{\mathrm{P}}) \cdot x_1 \\ &= \Big(h_{11}(\vec{r}_{\mathrm{P}}) - h_{11}(\vec{r}_{\mathrm{P}0}) - K_0\big(h_{21}(\vec{r}_{\mathrm{P}}) - h_{21}(\vec{r}_{\mathrm{P}0})\big)\Big) \cdot x_1 \end{aligned} \tag{9}$$

Again, $dh(\vec{r}_{\mathrm{P}}) = y(\vec{r}_{\mathrm{P}})/x_1$ can be formally evaluated as a function of the person's position and it can be seen as a signal sent out from the person with a varying amplitude. Nevertheless, $dh(\vec{r}_{\mathrm{P}})$ is a small quantity because it consists of two small quantities, see the comments after (7). This offers the advantage that the sensibility of the receiver can be kept high without running the risk of blasting it.

ADVANTAGES

The quantity $dh(\vec{r}_{\mathrm{P}})$ contains the calibration constant K_0, which depends on the full situation and includes all paths in our model. Once K_0 and the position $\vec{r}_{\mathrm{P}0}$ of the person at calibration as well as the antenna positions

are known, we can compute the expected signal $y(\vec{r}_P) = dh(\vec{r}_P) \cdot x_1$ for a fictive arrangement without any further knowledge of the other paths. Figure 2 gives an example showing a contour plot of the expected signal $|\mathrm{dh}(\vec{\mathrm{r}}_P)|$. The red point is the location of the person at calibration, while the black and the green point are the fixed locations of transmitting antennas and the blue point is the position of the receiver. All antennas are arranged in the drawing plane. The values shown as contours represent the expected signal if the person were at the respective position. If the person is moving away from the antennas, the signal will decrease, while close to the transmitters the signal increases.

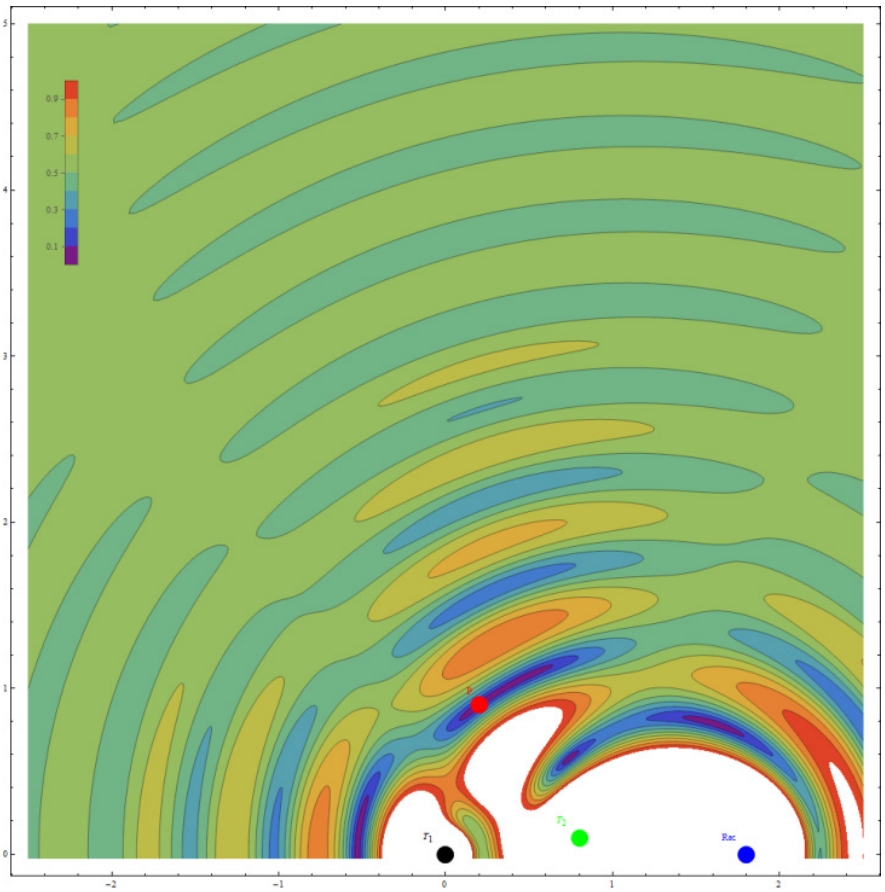

Figure 2: Example of a contour plot of the expected signal $|\mathrm{dh}(\vec{\mathrm{r}}_P)|$. The red point indicates the location of the person at calibration. The black and green points are the fixed locations of the transmitting antennas and the blue point is the receiver location. All antennas are arranged in the drawing plane.

The given coordinates are in units of wavelength. Note that the picture depends both on the calibration constant K_0 (which is arbitrarily set to $-0.9 + 0.3\mathrm{j}$) but also on the position $\vec{\mathrm{r}}_{P0}$ (the red point) and the positions of the antennas. Generally more than one zero can occur although zeros are at isolated points. The respective low value areas around a zero are typically narrow valleys. This means that a person moving along the valley is harder to be detected than a person moving across the valley.

Concerning the position $\vec{r}_{P0}$ (Position of person during calibration) another issue is important. Keeping in mind that the field of the transmitters shows some interference pattern it is clear that, depending on the value of the calibration constant K_0, the position $\vec{r}_{P0}$ might be at either a relative minimum or a relative maximum of the mentioned interference pattern. Consequently, the initial impact of the person on the calibration might be different and can lead to generally higher or lower signals even for other positions of the person.

COTS COMPATIBILITY

The simplicity of the single frequency sensing technique allows COTS components to be used when building the system. The digital signal processing, discussed in the next section, requires only FFT operations, simple operations with complex numbers and inversion of a 2×2-matrix. These are standard operations for digital signal processors. Furthermore, the transmitted signals can be generated by a (possibly tuneable) single frequency source.

DUAL POLARIZATION CALIBRATION

In this section, we describe the operations that are performed in the processing node of the single frequency sensing system in order to find the calibration state.

The received signal at the receiver antenna (Figure 1) can be described using the equation

$$R = \begin{bmatrix} R_{\mathrm{x}} \\ R_{\mathrm{y}} \end{bmatrix} = \begin{bmatrix} a & b \\ c & d \end{bmatrix} \begin{bmatrix} T_{\mathrm{x}} \\ T_{\mathrm{y}} \end{bmatrix} + \begin{bmatrix} e & f \\ g & h \end{bmatrix} \begin{bmatrix} C_{\mathrm{x}} \\ C_{\mathrm{y}} \end{bmatrix} = M_T T + M_C C \tag{10}$$

where M_T is the transmitter antenna transmission matrix, M_C is the calibration antenna transmission matrix and T and C are respectively the transmitter and calibration signals, each having two polarization denoted by the indices x, y. Note that in a typical setup and in the measurements presented below, $T_{\mathrm{x}} = 0$, i.e. no signal is sent on the x-polarization of the transmitter antenna.

Since the received signal is zero when the calibration is perfect, the calibration signals have to fulfil the condition:

$$M_T T + M_C C = 0 \tag{11}$$

This means that the ideal calibration signals are given by

$$C = -M_C^{-1} M_T T \tag{12}$$

where M_C^{-1} is the inverse of the calibration antenna transmission matrix.

To find the transmission matrices M_T and M_C, all but one components of T and C in (10) are set to zero while the remaining one is set to unity (i.e. only the corresponding polarizations of the transmitter and calibration antennas send a signal) and the received signals are measured, practically after performing an FFT on the received time domain signals. Each measurement yields a column of the matrices M_C or M_T.

For example, setting $T_{\mathrm{y}} = 1$ and measuring the received time signal $r_{\mathrm{x}}(t)$ on the x-polarization, the amplitude a_{x} and phase φ_{x} of the spectral component $R_{\mathrm{x}}(f)$ (where f is the frequency of the single frequency signal) relative to the transmitted signal leads to the entry

$$b = a_{\mathrm{x}} e^{j\varphi_{\mathrm{x}}} \tag{13}$$

of the transmission matrix M_T. The other matrix entries are obtained analogously. This calibration procedure to find the ideal calibration signals is performed in MATLAB and summarized in Figure 3.

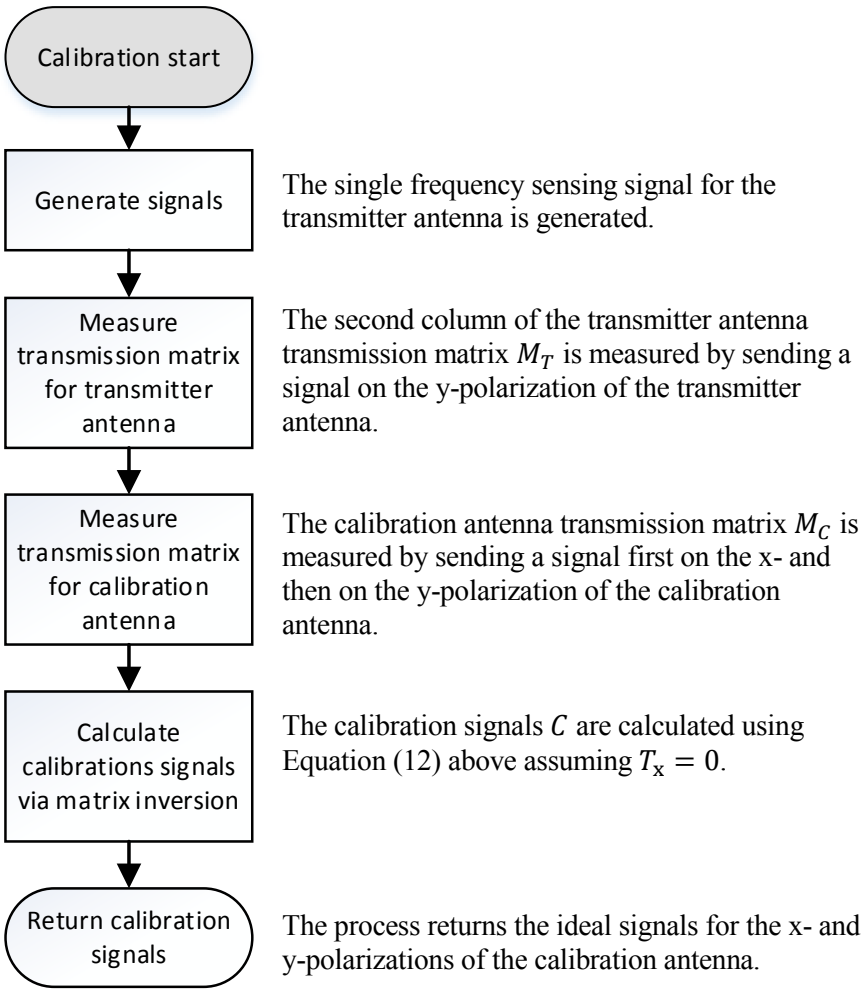

Figure 3: Flowchart of the calibration process.

TRACES AND SIMULATION RESULTS

In order to compare simulations and measurements more easily, we will consider the amplitude and phase variations along some predefined traces. In fact, we define three directions along which the object is moved. As depicted in Figure 4, the object will be moved from $\vec{r}_{P0} = (1.5,0.5)$ once to the left (negative X direction), once to the bottom (negative Y direction), and once to the bottom left (45 degree angle to the negative X and Y directions). In all three cases, the object is moved for one meter. For each of the simulations or measurement points, the amplitude and phase of the received signal are stored.

The simulation results are shown in Figure 4. Note that for simplicity, we have plotted only the amplitude results.

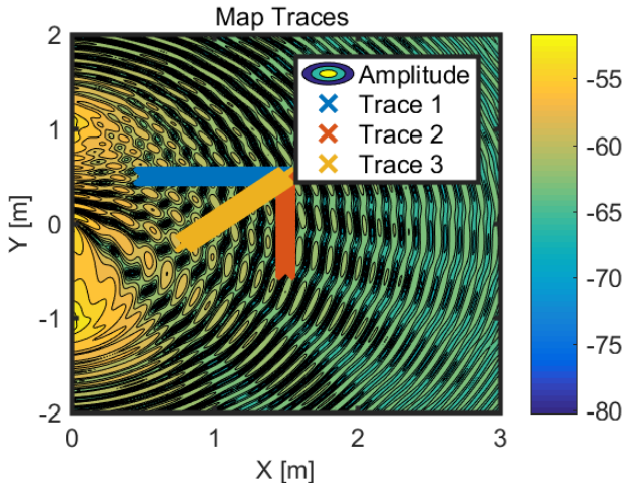

Figure 4: Traces for evaluation of simulations and measurements.

EXPERIMENTAL SETUP

In order to perform single frequency sensing measurements, the setup shown in Figure 5 is used. It consists of an arbitrary waveform generator (A), an oscilloscope (B), a PC to perform signal processing (C) and three antennas. Antenna D is the transmitter that sends the sinusoidal signal at a certain constant frequency f. The remaining signal after the calibration with the calibration antenna E is received by the receiver F. As discussed above, the calibration is achieved by transmitting appropriate signals from the calibration antenna E that cancel out the signal from the transmitter D. Note that in this setup, only the y-polarization is used in the transmitter D, while both polarizations are used for the other two antennas.

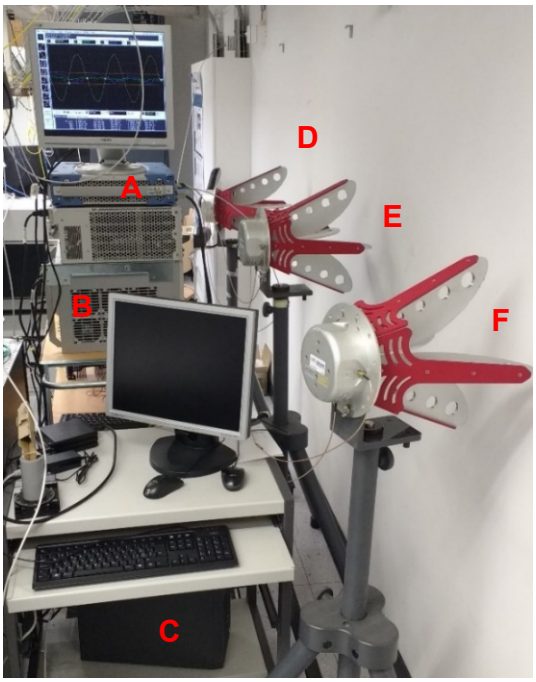

Figure 5: Picture of the receiver setup in the adjacent room with the three antennas (receiver (F) in the foreground, calibration (C) in the middle and transmitter (D) in the background), the arbitrary waveform generator (A) and the oscilloscope (B).

EXPERIMENTAL RESULTS

Measuring the amplitude of the frequency component at the system frequency f of the SFS system results in the plots shown in Figure 7. The measured curves in Figure 7 show a good agreement with the simulated curves in Figure 6, especially if one considers the simplifications of the simulation (isotropic antennas; transmitter, moving object and receiver are modelled as infinitesimally small points; scatterers are modelled as discrete elements).

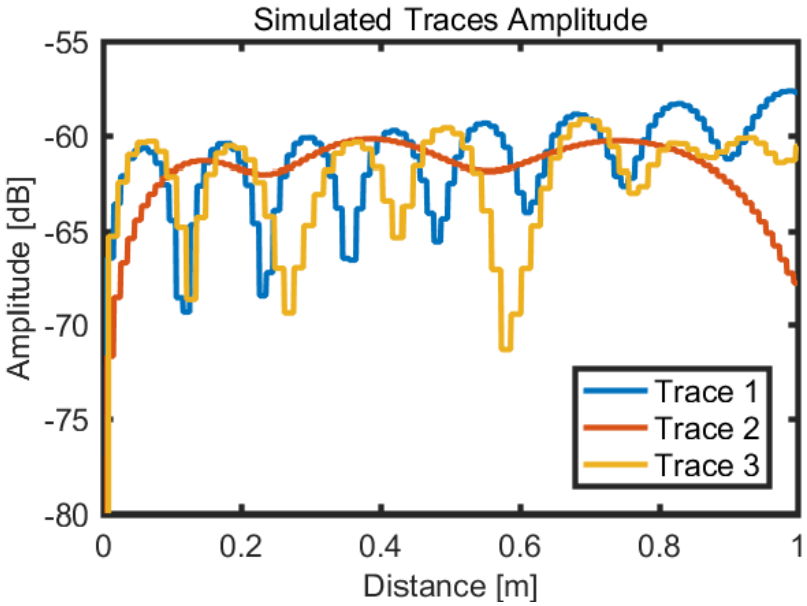

Figure 6 Simulated amplitude traces corresponding to traces shown in Figure 4.

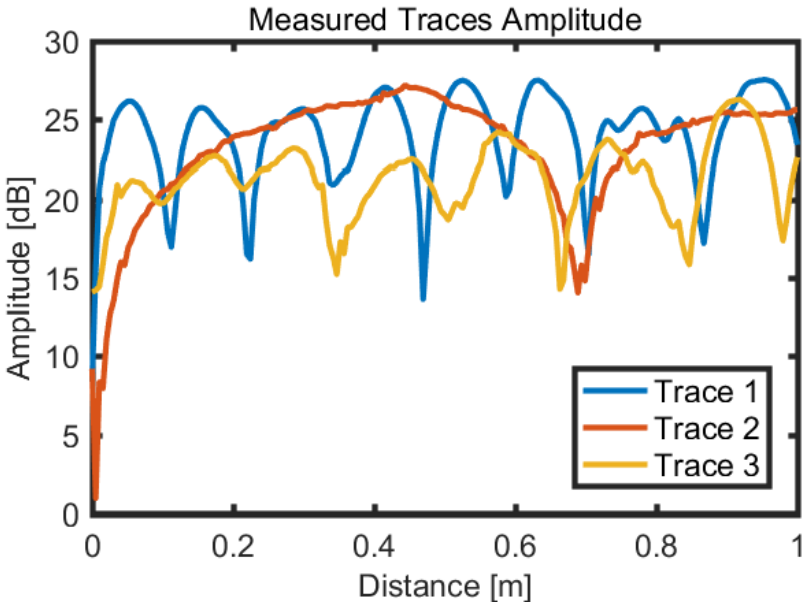

Figure 7: Measured amplitude traces.

These results have been obtained using the three pre-defined movement paths and therefore show different amplitude variations. Yet, evaluating a path direction from the amplitude ripples has shown to be a very complex task to solve.

MOVEMENT DETECTION RESULTS

To demonstrate the ability of the single frequency sensing system to detect human movement in a room, a simple experiment was performed. First, the dual polarization SFS calibration procedure as described above was executed. Then, the system started to monitor the amplitude and phase of the received signal over a period of three and a half minutes. 70 seconds after the monitoring started, a subject started crossing the room in parallel to the wall several times. The distance from the wall during the crossings was approximately two meters. Then, the movement was stopped, while the system continued to monitor the parameters for a little while longer.

As an indicator of movement, the absolute values of the amplitude of the signal received on both the x- and y-polarizations were then added together and plotted over time. The results can be seen in Figure 8. The human movement in the room, starting at the 70-second mark and ending at the 160-second mark indicated by the dotted red lines, is clearly detected by the system, as can be seen from the peaks in the plot. Fluctuations in the amplitude of the indicator are a result of 1) the movement of person through the room and 2) the valleys in the contour plot. In the future, a more sophisticated indicator, using both amplitude and phase information, could lead to improved detection performance.

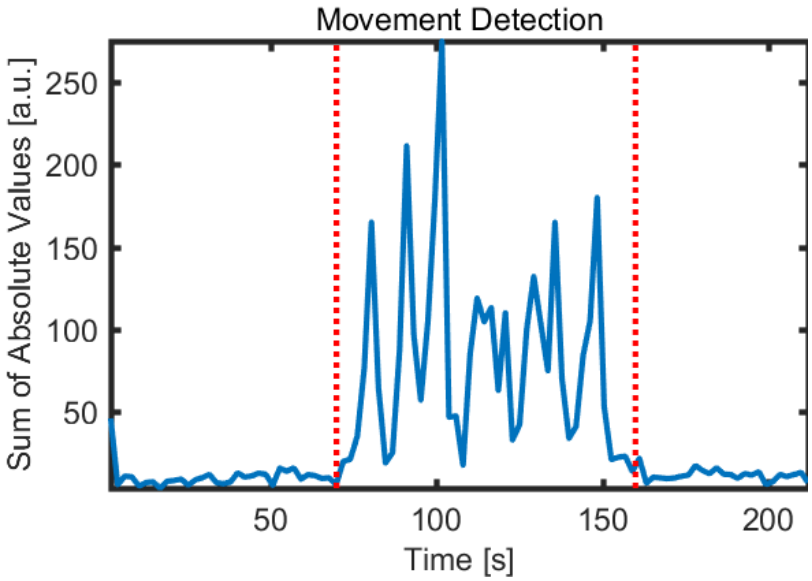

Figure 8: Plot of the measurement results for movement detection using single frequency sensing. The start and end of the movement at 70 seconds and 160 seconds are clearly visible and marked by the dotted red lines.

FURTHER WORK

The distance between the antenna and the wall will be increased in future measurements. With such a measurement, the quality of the results would also depend on the conditions of the room in which the sensor is located. Yet, by carefully choosing an antenna with an appropriate gain, the area of detection can be concentrated toward the remote wall and therefore the room of interest. Of course, crossing the field of view of the antenna on the sensor side would trigger a detection.

One of the key advantages of SFS should be its simplicity of implementation, as it only requires a function generator and a low speed acquisition board. In future work, we aim to implement the proposed concept using COTS components capable of being integrated into a handheld device. Another advantage of SFS for handheld devices is that the power consumption can be largely reduced by probing the room for short times (~1ms, i.e. more than 10^6 periods of the carrier) only a few times per second.

CONCLUSION

The findings reported in this letter show that dual polarization single frequency sensing is a very simple technique that can be used to detect movement in a room through a wall. The consideration of both polarizations reduces the disturbance caused by reflections, multipath propagation and scattering. Since only a single frequency is used for the sensing, the scheme is simple to implement and resilient to interference provided that the frequency of the system could be changed.

The measurements showed a good agreement with the simulations considering the simplified nature of the simulation environment. This means that algorithms for improved accuracy and extended capabilities of the SFS system could be developed and tested based on simulations, before being tested in the laboratory.

ACKNOWLEDGMENTS

armasuisse Science and Technology is acknowledged for funding of this project.

REFERENCES

[1] Lukin, K. and Konovalov, V., 'Through Wall Detection and Recognition of Human Beings Using Noise Radar Sensors', *RTO-MP-SET-080*, 2004, pp. 11-13.

[2] Montigny-leboeuf, A.D. and Massicotte, F., 'Passive Network Discovery for Real Time Situation Awareness', *RTO-MP-IST-041*, 2004, pp. 19-20.

[3] Palmer, J., Martorella, M., Littleton, B., and Homer, J., 'Using Emulated Bistatic Radar in Highly Coherent Applications : Overview of Results', *RTO-MP-SET-095*, 2006, pp. 1-10.

[4] Wu, S., Tan, K., Xia, Z., Chen, J., Meng, S., and Guangyou, F., 'Improved Human Respiration Detection Method Via Ultra-Wideband Radar in through-Wall or Other Similar Conditions', *IET Radar, Sonar & Navigation*, 2016, 10, (3), pp. 468-476.

[5] Li, J., Liu, L., Zeng, Z., and Liu, F., 'Advanced Signal Processing for Vital Sign Extraction with Applications in Uwb Radar Detection of Trapped Victims in Complex Environments', *IEEE Journal of Selected Topics in Applied Earth Observations and Remote Sensing*, 2014, 7, (3), pp. 783-791.

[6] Chen, X., Leung, H., and Tian, M., 'Multitarget Detection and Tracking for through-the-Wall Radars', *IEEE Transactions on Aerospace and Electronic Systems*, 2014, 50, (2), pp. 1403-1415.

[7] JalaliBidgoli, F., Moghadami, S., and Ardalan, S., 'A Compact Portable Microwave Life-Detection Device for Finding Survivors', *IEEE Embedded Systems Letters*, 2016, 8, (1), pp. 10-13.

[8] Gennarelli, G., Solimene, R., Soldovieri, F., and Amin, M.G., 'Three-Dimensional through-Wall Sensing of Moving Targets Using Passive Multistatic Radars', *IEEE Journal of Selected Topics in Applied Earth Observations and Remote Sensing*, 2016, 9, (1), pp. 141-148.

[9] Lagunas, E., Amin, M.G., and Ahmad, F., 'Through-the-Wall Radar Imaging for Heterogeneous Walls Using Compressive Sensing', in, *2015 3rd International Workshop on Compressed Sensing Theory and its Applications to Radar, Sonar and Remote Sensing (CoSeRa)*, (2015).

[10] Ahmad, F., Amin, M.G., and Qian, J., 'Through-the-Wall Moving Target Detection and Localization Using Sparse Regularization', in, (2012).

[11] Ralston, T.S., Charvat, G.L., and Peabody, J.E., 'Real-Time through-Wall Imaging Using an Ultrawideband Multiple-Input Multiple-Output (Mimo) Phased Array Radar System', in, *2010 IEEE International Symposium on Phased Array Systems and Technology*, (2010).

[12] Chen, Q., Chetty, K., Woodbridge, K., and Tan, B., 'Signs of Life Detection Using Wireless Passive Radar', in, *2016 IEEE Radar Conference (RadarConf)*, (2016).

[13] Pastina, D., Colone, F., Martelli, T., and Falcone, P., 'Parasitic Exploitation of Wi-Fi Signals for Indoor Radar Surveillance', *IEEE Transactions on Vehicular Technology*, 2015, 64, (4), pp. 1401-1415.

[14] Chetty, K., Smith, G.E., and Woodbridge, K., 'Through-the-Wall Sensing of Personnel Using Passive Bistatic Wifi Radar at Standoff Distances', *IEEE Transactions on Geoscience and Remote Sensing*, 2012, 50, (4), pp. 1218-1226.

[15] Adib, F. and Katabi, D., See through Walls with Wifi!', *Proceedings of the ACM SIGCOMM 2013 conference on SIGCOMM*, (ACM, 2013).